3rd URSI AT-AP-RASC, Gran Canaria, 29 May – 3 June 2022

Radio Frequency Interference Detection in Microwave Radiometry: A Novel Feature-Based Statistical Approach

Imara Mohamed Nazar* and Mustafa Aksoy
Electrical and Computer Engineering Department
University at Albany, SUNY, Albany, NY, USA
Emails: {imohamednazar, maksoy}@albany.edu

Abstract

The amount of radio frequency interference (RFI) present in microwave radiometer observations is significantly increasing over time. The presence of RFI in radiometer measurements impacts the computation of crucial geophysical parameters of the Earth's surface and atmosphere. In this paper, we introduce the idea of using heterogeneous feature–based representation for baseband radiometer measurements. The feature values are estimated empirically using statistical methods such as maximum likelihood estimator (MLE) and Monte Carlo experiments. Further, we also implement a feature selection algorithm that selects the most discriminant features. The proposed approach reviews the features sequentially to determine the final decision based on maximum a posteriori (MAP) estimation. The performance evaluation of the proposed approach with the traditional RFI detection methods shows that the proposed approach has a higher ability to detect RFI even when the interference to noise ratio (INR) of the RFI is as low as -20 dB.

1 Introduction

The observations from the passive microwave sensors are the primary components to quantify and predict the weather and atmospheric dynamics [1]. The RFI in these passive remote sensing measurements is continuously increasing over time due to the exponential growth in telecommunication systems. Hence, the accuracy of the radiometric measurements and the accurate retrieval of critical geophysical parameters become questionable. Most of the existing detection studies are solely dependent on a single characteristic of the radiometer measurements, i.e., time, frequency, statistical, etc (e.g., [2, 3]). Even though they performed well in experimental studies that contain a single type of RFI, they do not consider the co–existence of different types of RFI. Addressing these shortcomings, in our previous work, we have introduced RFI detection techniques that can combine the information from several domains simultaneously to detect the RFI contamination in a measurement [4-6]. In this paper, we propose a novel, feature–based, statistical approach to detect RFI in microwave radiometry. In contrast to the state–of–the–art multidimensional methods, the proposed approach can analyze multiple discrete domains simultaneously. A statistical feature selection method is also proposed to identify the significant signal characteristics (features) that improve the performance of the detection process. To demonstrate the effectiveness of the proposed approach, we have compared the proposed approach with traditional RFI detection methods.

2 Bayesian Detection Approach

Consider a set $\mathcal{R}$ of radiometer measurements where each measurement $r_i, i = \{1,2,\cdots,N\}$ is described by d number of feature values, namely f_{in}, $n = \{1,2,\cdots,d\}$. The Bayesian detection [7] approach is formulated as a binary hypothesis testing problem where r_i may belongs to one of two hypotheses, i.e., RFI–contaminated ($H_{\mathcal{C}}$) and RFI–free ($H_{\mathcal{N}}$). For each feature value f_n, the probability $P(f_n|H_{\mathcal{C}})$ (similarly $P(f_n|H_{\mathcal{N}})$) of the evaluation of *nth* feature is when the true hypothesis is $H_{\mathcal{C}}$ (similarly for true hypothesis $H_{\mathcal{N}}$) is calculated from the training data. Further, the *a priori* probabilities $P(H_j)$ of measurement r_i belongs to the class of $j = \{\mathcal{C},\mathcal{N}\}$ is also estimated empirically. In this method, for each measurement r_i, we are interested in computing the posterior distribution $P(H_j|r_i)$ via Bayes' theorem which, uses the class conditional distribution of each feature and the prior distribution of the data. In order to simplify the problem, we have assumed that the features are conditionally independent given the class label. The final prediction output is estimated using the MAP method as $\hat{y}_i = \arg\max_{j=\{\mathcal{C},\mathcal{N}\}} P(H_j|r_i)$.

3 Data Generation

The RFI-free radiometric measurements follow a zero–mean Gaussian distribution with a uniform power spectrum [8]. Hence, we modeled the RFI–free radiometer measurements as zero-mean white Gaussian noise. The RFI caused by the man–made signal is additive to the naturally occurring thermal noise, and it causes a bias in the RFI–free radiometer measurements. Therefore, we simulated the RFI–contaminated measurements by adding the interference signal to white Gaussian noise. In particular, we

Table 1. The list of extracted features

Time Domain	Statistical Domain		Spectral Domain
	Standard Moments & other	Normality Tests	
Mean	Skewness (m_3)	Jarque–Bera (JB) test	Spectral mean
Variance	Kurtosis (m_4)	Lilliefors (L) test	Spectral variance
Power	$m_5 - m_{10}$	Anderson–Darling (AD) test	Spectral maximum
Peak to peak distance (PPdist)	Inter quantile range (IQR)	Ljung–Box (LB) test	Spectral entropy
Median			Spectral distance
Average over absolute value of first differences (meanAbsDiff)			Spectral skewness
Average over time series differences (meanDiff)			Spectral kurtosis
Mean of the auto-correlation coefficient (meanACC)			
Distance			

use the pulsed sinusoidal interference signal because of its ability to create short pulses (low DC) and continuous contamination (high DC) [9]. The amplitude, frequency, pulse repetition interval, and the phase shift of the sinusoidal signal are set to 1 V, 12 MHz, 300 μ s, and 0 degrees, respectively. This study aimed to evaluate the performance of the proposed approach with DC and INR of the interference signal. Hence, interference signals with different DC and INR are generated by varying the DC from 1% to 100% in increment of 1% and INR from -20 dB to 10 dB in the step of 1 dB. The sampling rate and the integration time are set similar to the SMAP radiometer with corresponding values of 96 MSPS and 300 μ s, respectively. We have extracted twenty–nine features in time, frequency, statistical, and spectral domains. The extracted features are summarized in Table 1.

4 Bayesian Detection Implementation

The Bayesian detection implementation steps are illustrated in Figure 1. As shown in the figure, both RFI–free and RFI–contaminated radiometer measurements are generated as described in section 3. The features listed in Table 1 are extracted from each radiometer measurement and organized in a row to construct the data matrix. Here, we have constructed 3100 such datasets associated with each pair of INR and DC values. The most discriminant features are selected based on the error static derived from the sum of type I and type II errors. Next, the data matrix is divided into two parts, i.e., training and testing. The data

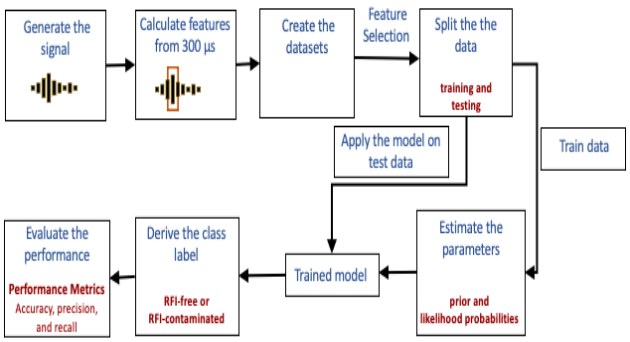

Figure 1. Steps followed by the Bayesian detection

contained in the training set is used to train the Bayesian detection model that outputs the training parameters such as prior and likelihood probabilities. Finally, the trained Bayesian detection model is evaluated on the test data. To avoid overfitting, we have used a cross–validation technique, namely five–fold cross-validation. The data matrix is divided into five folds of approximately equal size. Each fold is treated as a validation set for the model trained on the remaining four–folds. Thus, each fold of 160 measurements is tested by a model trained on the remaining 640 measurements. The performance of the proposed approach in each fold is evaluated using performance metrics, namely accuracy, precision, and recall, and averaged over the number of folds. The metric accuracy is the fraction of correctly predicted measurements out of the total number of measurements. Here, the number of correctly predicted measurements indicates the addition of the numbers of RFI–contaminated measurements that are predicted as RFI–contaminated and the RFI–free measurements that are predicted as RFI–free. The precision gives the fraction of correctly predicted RFI–contaminated measurements from the total number of the measurements that are predicted as RFI–contaminated. The total number of the measurements that are predicted as RFI–contaminated also includes the RFI–free measurements that are predicted as RFI–contaminated. The recall metric is the fraction of correctly predicted RFI–contaminated measurements from the total number of RFI–contaminated measurements in the dataset.

5 Results

5.1 Feature Selection

Here, we have computed the summation of the type I and type II errors and ranked the features based on the combined error static to select the most discriminant subset of relevant features. Figure 2(a) shows the best discriminating feature in all the INR and DC RFI cases. The feature that appears in most of the high INR RFI cases (i.e., blue color in the diagram) is variance. The features primarily show up in the RFI cases with INR ≤ -5 dB (followed by the blue region) and the INR > -5 dB with DC $\leq 40\%$ are spectral variance, spectral entropy, and spectral maxi-

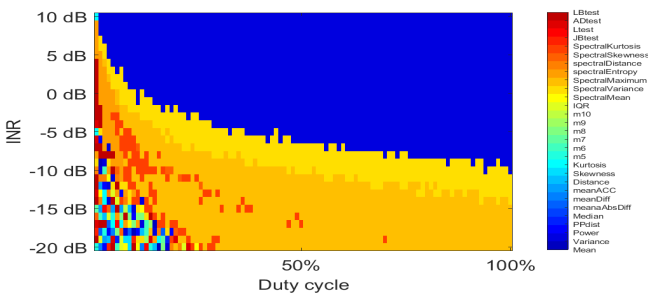

(a)

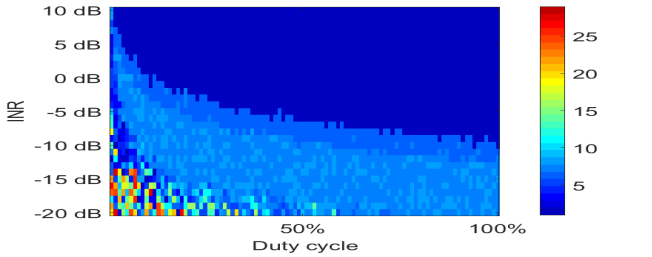

(b)

Figure 2. Best discriminating feature (a) and the feature ranking of the variance (b) as a function of INR and DC.

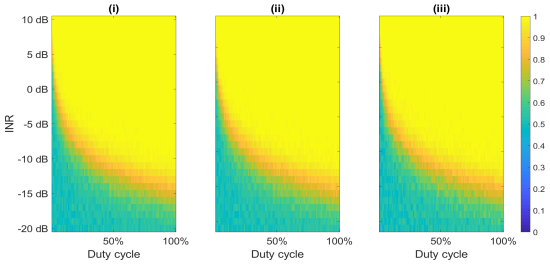

(a)

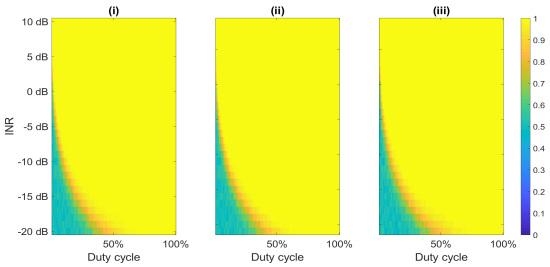

(b)

Figure 3. Accuracy (i), precision (ii), and recall (iii) of the Bayesian detection with two features (a) and additionally introduced features (b) as a function of INR and DC.

mum. The features that appear in red in the yellow regions are spectral kurtosis and spectral skewness. The normality test, specifically, the LB test, performs well in the RFI cases with DC=1% and INR=[−5 dB, 0 dB]. In summary, the time domain features are more dominant in high INR and high DC RFI cases. The spectral features show a significant performance in all the other cases except for the RFI cases with low INR and low DC. Normality tests work well when the DC is very low such as 1%–5%. There are no specific groups of features observed in the very weak RFI cases (i.e., datasets with low INR and low DC). To select the other features, we have plotted the ranking of each feature in all the INR and DC RFI cases. Figure 2(b) shows the feature ranking (i.e., rank one implies that the feature outputs the lowest error) of the variance as a function of INR and DC. As seen in the figure, variance is the best feature in most of the high-INR RFI cases than in low-INR RFI cases. By performing a similar analysis on all the available features, we have shortlisted the following features, namely variance, power, kurtosis, mean of the absolute value of first differences, mean of the autocorrelation coefficient, spectral variance, spectral maximum, spectral entropy, spectral skewness, spectral kurtosis, and the LB test.

5.2 Bayesian Detection Performance

The performance of the Bayesian detection approach with two features (a) and eleven features (b) are shown in Figure 3. As seen in Figure 3 (a), even with two features, Bayesian detection achieves more than 90% of accuracy, precision, and recall for low INR cases such as INR = −15 dB depending on the value of the DC. The performance is even more improved, i.e., nearly 100% of accuracy, precision, and recall is observed for very low INR cases such as INR = −20 dB (see Figure 3 (b)) with the addition of new features using our novel feature selection algorithm. These observations highlight the importance of introducing more meaningful features.

5.3 Performance Comparison with Baselines

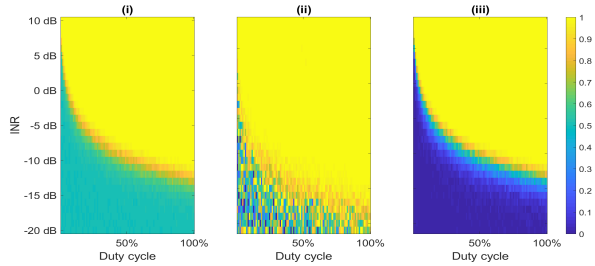

Figure 4. Accuracy (i), precision (ii), and recall (iii) of the OR method as a function of INR and DC.

In this work, we have compared the performance of the proposed RFI detection method with the widely used traditional RFI detection method, i.e., we combined the detection outputs from kurtosis detection and pulse blanking for the maximum likelihood of detection. Specifically, the measurement is flagged as RFI–contaminated if the RFI–contamination is detected by at least one of the methods (we will refer this method as “OR method”). Figure 4 shows the accuracy, precision, and recall values of the OR method as a function of INR and DC. Further, we have compared the performance of the Bayesian detection with OR method by subtracting the performance metrics of the OR method from Bayesian detection. Figure 5 shows the accuracy, preci-

sion, and recall differences between the Bayesian detection and OR method as a function of INR and DC. In particular, Figure 5 (a) shows the performance difference when the Bayesian detection is implemented with two features (i.e., power and kurtosis).

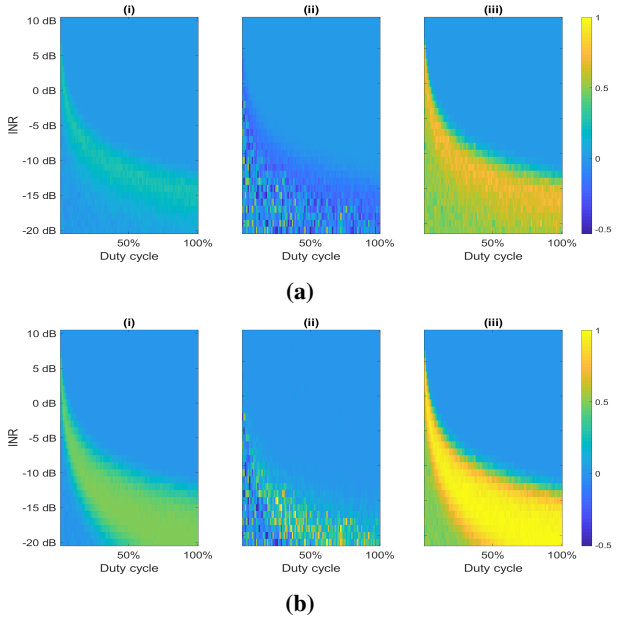

(a)

(b)

Figure 5. Accuracy (i), precision (ii), and recall (iii) difference between the Bayesian detection and OR method with two features (a) and additionally introduced features (b) as a function of INR and DC.

Figure 5 (b) shows the performance difference between Bayesian detection and OR method when the Bayesian detection implemented with eleven features that are shortlisted in section 5.1. As seen in Figure 5 (a), compared with OR method, the Bayesian detection with power and kurtosis achieves higher accuracy and recall even for lower INR cases, i.e., INR ≤ -12 dB, depending on the value of DC. Specifically, higher recall values, i.e., the fraction of the detected RFI-contaminated measurements out of all RFI-contaminated measurements, in low INR cases indicate that Bayesian detection performs better in detecting RFI contamination from all the available RFI–contaminated measurements than OR method. From Figure 5 (b), we can see that with the addition of more meaningful features, there is a considerable amount of accuracy, precision, and recall increase observed in lower INR cases.

6 Conclusions and Future Work

In this paper, we proposed a Bayesian technique to detect the RFI in microwave radiometry. We described each radiometer measurement using twenty-nine features that characterize the simulated RFI environment in time, frequency, and spectral domains. Furthermore, we have implemented a feature selection algorithm to select the subset of relevant features that maximize the mutual information between the selected features and the class variable. In order to implement the Bayesian detection, we derived the MLE of unknown parameters such as class conditional likelihood estimate of the features and prior distribution, empirically, from the data. The evaluation results with two features (i.e., power and kurtosis) show the ability of the Bayesian detection to perform well than the state–of–the–art OR method that uses the same features. The results also highlight the importance of the feature selection algorithm such that there is a significant improvement observed in the performance by increasing the number of meaningful features. In our future work, we plan to extend this study to detect different types of RFI. We also plan to implement the proposed approach on real radiometer data. Finally, we will test the feasibility of the proposed algorithm in hardware.

References

[1] (U.S.) National Research Council, “Spectrum Management for Science in the 21st Century,” *National Academies Press*, 2010.

[2] R. D. De Roo and S. Misra, “ Effectiveness of the Sixth Moment to Eliminate a Kurtosis Blind Spot in the Detection of Interference in a Radiometer,” *IGARSS - IEEE International Geoscience and Remote Sensing Symposium*, **2**, July 2008, pp. 331–334.

[3] B. Guner, J. T. Johnson, and N. Niamsuwan, “Time and Frequency Blanking for Radio-frequency Interference Mitigation in Microwave Radiometry,” *IEEE-Transactions on Geoscience and Remote Sensing*, **45**, 11, November 2007, pp. 3672–3679.

[4] I. M. Nazar, M. Aksoy, “Radio Frequency Interference Detection in Microwave Radiometry Using Support Vector Machines,” *URSI GASS 2020*, 2020.

[5] I. M. Nazar, M. Aksoy, “Radio Frequency Interference Detection in Microwave Radiometry Using Support Vector Machines,” *Radio Science Letters*, **2**, 2020.

[6] I. M. Nazar and M. Aksoy, “Radio Frequency Interference Detection in Microwave Radiometry Using Density Based Spatial Clustering," XXXIV th URSI GASS, 2021, pp. 1-4, doi: 10.23919/URSI-GASS51995.2021.9560303.

[7] K.P. Murphy, “Machine learning: a probabilistic perspective”, *MIT press*, 2012.

[8] R. D. De Roo, S. Misra, and C. S. Ruf, “Sensitivity of the Kurtosis Statistic as a Detector of Pulsed Sinusoidal RFI,” *IEEE Transactions on Geoscience and Remote Sensing*, **45**, no. 7, pp. 1938-1946, July 2007, doi: 10.1109/TGRS.2006.888101.

[9] S. Misra, “Development of radio frequency interference detection algorithms for passive microwave remote sensing,” *Ph.D. dissertation, University of Michigan*, Jan. 2011.